LMU LUDWIG-MAXIMILIANS-UNIVERSITÄT
TECHNISCHE UNIVERSITÄT MÜNCHEN TUM

Institute of Bioinformatics and Systems Biology
Helmholtz Center Munich; computational modeling in biology

Bachelorarbeit
in Bioinformatik

A quantitative model to study the role of pitchfork and the primary cilium in the hedgehog signaling pathway

Cedric Landerer

Aufgabensteller:	Prof. Dr. Fabian Theis
Betreuer:	Dr. Dominik Lutter
Abgabedatum:	15.07.2011

Ich versichere, dass ich diese Bachelorarbeit selbständig verfasst und nur die angegebenen Quellen und Hilfsmittel verwendet habe.

15.07.2011 _____

Cedric Landerer

Contents

Abstract

Sonic hedgehog (Shh) controls the early development of embryonic cells in vertebrates and is conserved over many taxa. Sonic hedgehog is secreted by a signaling cell into the extracellular matrix. Shh binds to the receptor protein Patched (Ptc) that is placed in the plasma membrane of the receiving cell. So the Shh signal is transduced into the cell. Here we introduce two quantitative models based on ordinary differential equations (ODE) to simulate and analyze the Shh signal pathway. At the end we will show which model describes the data most likely. We will present the data and how it is processed for the training. The models are trained on experimental data by a simulated annealing approach. We also include Pifo to the models. Pifo is assumed to be important for ciliary trafficking. We analyze the role of Pifo in the Shh signaling pathway with the ODE models presented in this work and will show that Pifo does enhance the expression of the Shh target genes by turning Pifo off. So we can compare the results of the fitting and the prediction.

Zusammenfassung

Sonic hedgehog (Shh) ist verantwortlich für die Kontrolle der frühen Entwicklung von embryonalen Zellen in Vertebrata. Shh ist dabei über viele Taxa konserviert. Shh wird von einer signalisierenden Zelle in die extrazelluläre Matrix sekretiert wo es dann an das Rezeptorprotein Patched (Ptc) bindet. Durch das binden an Ptc wird die Inhibierung von Smo durch Ptc aufgehoben und das Shh-Signal kann in die Zelle induziert werden. Wir werden in dieser Arbeit zwei quantitatives Modell, basierend auf ODE's vorstellen um den Shh Signalweg zu simulieren und zu analysieren. Zum Schluss wird wiedergegeben welches Modell am wahrscheinlichsten für eine Erklärung der Daten sorgt. Wir werden die zur Verfügung gestellten experimentellen Daten vorstellen und aufzeigen wie sie zum trainieren der Modelle verwendet wurden. Die Modelle wurden mit Hilfe einer Simulated Annealing Methode auf die experimentellen Daten trainiert. Wir haben den Shh Signalweg um Pifo ergänzt, ein Protein welches sich für den Transport ins Cilium verantwortlich zeigen soll. Ziel ist es die Rolle von Pifo im Shh Signalweg mit Hilfe der bereitgestellten ODE-Modelle zu analysieren. Dabei werden wir zeigen das Pifo die Expression der Gene welche auf das Shh-Signal reagieren verstärkt. Dafür wurde Pifo eliminiert um die Ergebnisse mit und ohne Pifo im System vergleichen zu können.

Chapter 1

Introduction

The hedgehog (Hh) signaling pathway plays a major role in the early development of embryonic cells, but is not understood in detail yet. The hedgehog signaling pathway is responsible for the growth, patterning and morphogenesis of many different regions within the body plans of vertebrates and insects[1]. The hedgehog pathway is present in most organs and tissues of the most vertebrates and is conserved over many taxa which shows its important role. For example, in Drosophila, hedgehog plays a role in larval body segment development. In annelid (also called 'ringed worms') it is involved in the segmentations process. Therefore it is important to understand this pathway in detail. In 2010 Pitchfork (Pifo) was discovered which also plays a role in the hedgehog signaling pathway. Pifo is a protein that is associated with ciliary targeting complexes and accumulates at the basal body during cilia disassembly[2]. To understand the role of Pifo, we created a quantitative ODE-model based on the current knowledge and trained on western blot data given from our collaborators. We want to answer the question, what the role of Pifo in the hedgehog pathway is and if it is responsible for ciliary trafficking.

1.1 The mechanism of the hedgehog pathway

Sonic hedgehog (Shh), a member of the hedgehog protein family, binds after secretion by a signaling cell to a receptor placed in the plasma membrane of the primary cilium of the receiving cell called Patched (Ptc)(Figure 1.1). Shh and Ptc form a complex which then is internalized. Ptc is a transmembrane protein with five extracellular and seven cytoplasmic regions. It is expressed in several tissues like brain, lung, liver and heart. The cilium is a sensorial organelle found in eukaryotic cells. The Patched protein represses the function of the signal transducer Smoothened (Smo) in the absence of Shh. Smo is a seven-pass transmembrane protein[6] and G-protein coupled receptor. It has a shorter extracellular domain of around 200 amino acids and a longer cytoplasmic domain of around 500 amino acids. If Shh binds to Ptc, the repression of Smo ends and the Shh signal is transduced to the cytoplasm[3].
In absence of the Shh signal, the target genes of Shh are repressed. As activator and repressor for the Shh target genes, the Gli protein family has been identified. The Gli

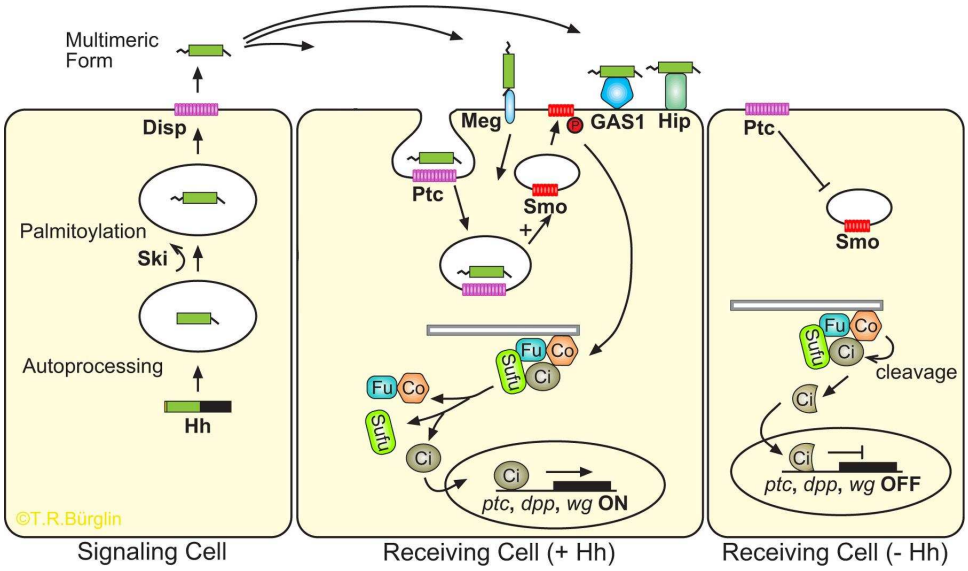

Figure 1.1: The sonic hedgehog pathway. (Left panel) Shh is autoprocessed and modified by Ski and then released by Disp into the extracellular matrix. (+Hh) Shh binds to Ptc present in the membrane which is then internalized. Now Smo can enter the membrane and the Shh signal is transduced. Cos2 is released from the microtubules and the Cos2/Fu/Su(fu)/Ci complex releases Cubitus interruptus (Ci) which is then translocated to the nucleus to activate the transcription of the target genes. (-Hh) Ptc inhibits the Smo and the Cos2/Fu/Su(fu)/Ci complex remains at the microtubules and Ci is cleaved by Cos2. The cleaved Ci acts as a repessor.[6].

family is a group of zinc finger transcription factors which are associated with the Shh signaling pathway. There are three members of this family present in vertebrates[4], Gli1, Gli2 and Gli3. With an active Shh signal, Gli1 is processed by phosphorylation into an active form (GliA) in the cilium. The activated Gli is then translocated into the nucleus where it acts as a transcription factor. Gli2 also acts as a transcription factor. Gli3 exists in two forms. In a full length form (Gli3) that acts as an activator after phosphorylation and translocation into the nucleus, and in a shorter C-terminally truncated form which acts as a transcriptional repressor (GliR). The cleavage is inhibited by Shh. Without Shh, Gli3 is phosphorylated by the Protein Kinase A (PKA) and then bound to the ubiquitin ligase β-TrCP[4].
Pifo is now propagated to be an adapter protein which is important for ciliary trafficking[2].

1.2 Motivation

The motivation of this work is to provide a quantitative model to clarify the role of Pifo in the Shh signal pathway. The Shh signaling pathway is not yet understood in detail, and the role of Pifo in the pathway is absolutely unclear yet. We want to answer mainly the question, what is the function of Pifo and the primary cilium in the Shh pathway.

Therefore, we created different models based on ordinary differential equations (ODE) with and without the differentiation between cytoplasm and cilium. We tested how the models will act with and without Pifo in its assigned role as an adapter protein for ciliary trafficking. So Pifo should enhance the system. Another question which came up during the work was about how the interaction between Smo and Ptc happens. We also tried to address this question. There are two possibilities known to us, one at which Ptc inhibits the import of Smo into the membrane and one where Smo and Ptc are both placed in the membrane. We have the chance to address this question also, just by taking the compartmentation into account(see. Section 2.2). Lai et. al published a one compartment ODE-model to investigate the function of the Shh pathway as a genetic switch[17]. They do not take the ciliary trafficking into account. Also we want to include Pifo in our system to investigate the role of Pifo in the Shh pathway.

Chapter 2

Methodology

We first did a literature search to understand the known mechanisms of the Shh signaling pathway to create two initial models which are both contain two compartments. They both included the trafficking of all proteins, but as this model was to complicated, detailed and also contained a lot of unmeasured protein, we decided after a discussion with our collaborators to start again. This time with a simple model, just containing the basic players. So we could extend this model if necessary. One advantage over the initial models was to get rid of a lot of unmeasured proteins in the model.

We used an ODE-approach to define the model of the Shh system because the progression of chemical and biochemical reactions are well described by mathematical equations. And as the derivative of a function provides the rates at which the equation is changing, we assumed that an ODE-model will characterize the Shh signaling pathway well.
First we created a new initial model without any compartmentation (see Section 2.2). This model was the base for further exploration. With just one compartment, we could also address the question about the interaction between Smo and Ptc. If Ptc inhibits the function of Smo by binding, the inhibition of Smo by Ptc is done by an interaction in the membrane[3]. Therefore we canceled Smo in the one compartment model out by setting it to the ShhPtc-complex (Figure 2.1). A 1:1 relation between Ptc and Smo is assumed here. For the other case a two compartment model was created which takes the import of Smo into the cilium in to account. Here we used a logistic function to model the dependency of the Smo import by Ptc, so this would be a non-binding inhibition. We will describe this in detail in Section Section 2.2.

The one compartment model causes numerical issues because we relinquish GliA to keep this model as simple as possible. From there we added GliA also to the one compartment model. We will describe this in detail in Section 2.2

2.1 Data

The data we used for the parameter training was provided by our collaborators from the group of Dr. Heiko Lickert.
For Gli1 we had 3 time courses with 7 time points. 2 time courses with 7 and 6 time

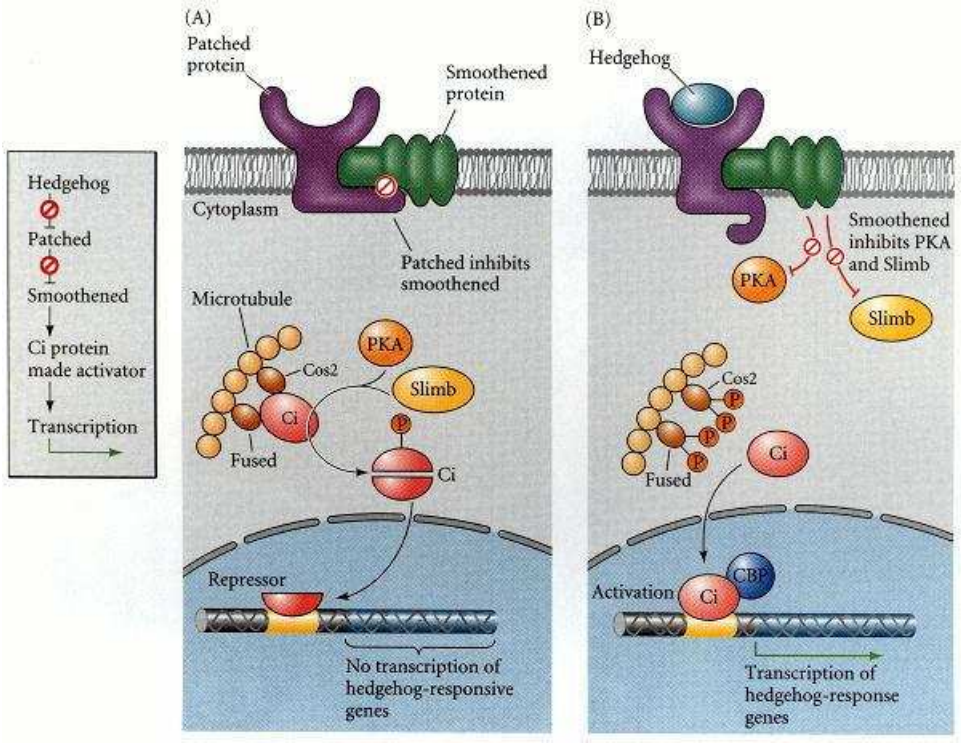

Figure 2.1: Illustration of a simplified possible inhibition mechanism of Ptc on Smo. The Gli family is condensed to Cubitus interruptus (Ci). There is no distinction between Gli1 and Gli3 shown. (A) Without Shh, Ci is phosphorylated by Protein Kinase A (PKA) and cleaved into the repressor by supernumerary limbs (Slimb), because Ptc inhibits the function of Smo. So, no transcription of the Shh responsive genes take place. Both proteins - Ptc and Smo - are present in the membrane and interacting directly. With an active Shh signal, the inhibition of Smo sag. So Ci is no longer cleaved into the repressor and an activation of the responsible genes can take place[3].

points for GliR, and for Pifo and Gli3 we had 1 time course, each with 7 time points. All datasets are in a range of 24h. We had data for the time points 0h, 0.5h, 1h, 2h, 4h, 6h and 24h after Shh induction. The raw data is shown in Figure 2.2.
For the later model training we calculated the mean μ and the standard deviation σ for each time point of Gli1 and Gli3 and assumed that Gli1 and Pifo share the same σ and Gli3 and GliR as well, because we were not able to calculate a standard deviation of Pifo and Gli3 from just one time course. For Gli3 and GliR this assumption is made because of the conservation of mass should keep the standard deviation at the same scale. In the case of Gli1 and Pifo, as we had to estimate a standard deviation, we used the one of Gli1 just because the expression of the proteins are in the same range.

The normalized data is shown in Table 2.1 and Table 2.2. In Figure 2.3 also the rescaled data is shown. For GliR we have a systematical shift in the data due to a different reference point. We corrected this shift by normalizing the data. Shh is induced at time point 0h. As we have no absolute molecule count, all concentrations are on an

time(h)	$Gli1_1$	$Gli1_2$	$Gli1_3$	$Gli1_{mean}$	$Pifo$	σ $Gli1/Pifo$
0	1773.437	1856.319	2685.249	2105.015	1282.234	504.201
0.5	4300.246	3888.75	4523.166	4237.387	11452.19	321.845
1	6264.581	6204.306	6718.516	6395.801	26273.56	281.01
2	8037.702	8115.743	8519.3	8224.248	27776.63	258.484
4	17823.72	11894.83	11261.46	13660	21662.96	3619.76
6	18644.56	20678.84	19200.02	19507.81	13258.06	1051.48
24	48829.57	40477.33	51214.99	46840.63	5375.853	5638.37

Table 2.1: The normalized time courses of Gli1, Pifo, and the respective standard deviation and mean.

time(h)	$Gli3$	$GliR_1$	$GliR_2$	$GliR_{mean}$	σ $Gli3/GliR$
0	4671.146	8052.794	9348.136	8700.465	915.944
0.5	6297.095	9960.986	10593.97	10277.48	447.59
1	7025.409	12421.11	11037.47	11729.29	978.38
2	16242.94	12547.74	12064.24	12305.99	341.889
4	21952.39	13373.69	11816.51	12595.1	1101.09
6	18433.37	14902.11	———	10754.34	1626.42
24	9209.167	3145.397	6386.233	4765.815	2291.61

Table 2.2: The normalized time courses of Gli3, GliR and the respective standard deviation and mean.

arbitrary scale. The $\sigma's$ were later used for the calculation of the likelihood.
Because in the second time course of GliR the time point at 6h is missing, we calculated the standard deviation for this time point by combining the time point 6 hour from time course one with the means of the time point 4h and 24h. With these 3 points, we were able to calculate a mean μ and a standard deviation σ. But because the standard deviation was significant larger as the other σ of the time course, we calculated the mean over all standard deviations of the time course $GliR_2$. So we got a σ in the same range as the data points from which we derived the σ.

After Shh induction, we see a change of the equilibrium in the cleavage reaction of Gli3. The equilibrium which is on the GliR site, is changing towards Gli3 (figure 2.2 B/D). This may have two reasons. First is, that the ShhPtc complex or Smo inhibits the cleavage, which is the most common reason, the second is that the Shh signal is stimulating the Gli3 transcription. It is yet unclear whether the ShhPtc or Smo inhibits the cleavage by inhibiting the PKA. We first tried both variants, but with respect to our collaborators we decided to use the variant with Smo as the inhibitor. The data shows that there is still a production of GliR while the Shh signal is active. So there is no complete shut down of the inhibition by GliR.

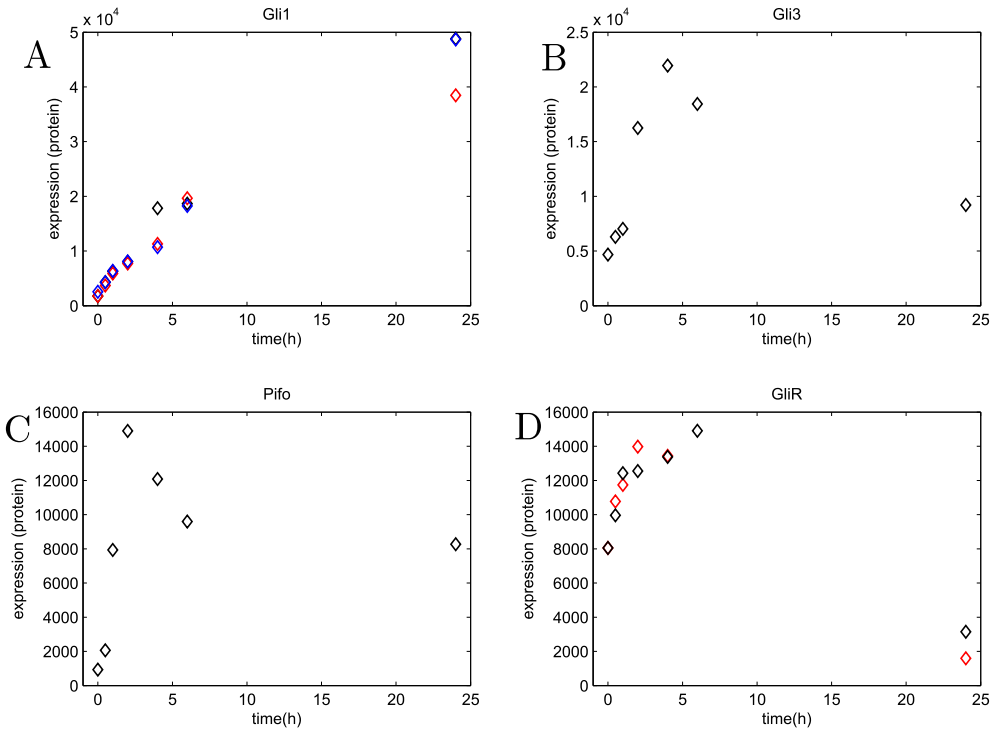

Figure 2.2: Shows the raw data of Gli1(A), Gli3(B), Pifo(C) and GliR(D). (A) The three time courses for Gli1. They show a small deviation in the first 4 hours and an increasing deviation in the later hours. (B) One time course for Gli3. After Shh activation (0h), one can find a substantial increase of the Gli3 concentration which should be due to the changing of the equilibrium. (C) For Pifo, also just one time course is available. One can see a sizable increase in the early hours until 2h, after that, Pifo decreases to a mid level. (D) Two time courses are available for GliR. One can see a notable increase at the beginning and a decrease in the later hours.

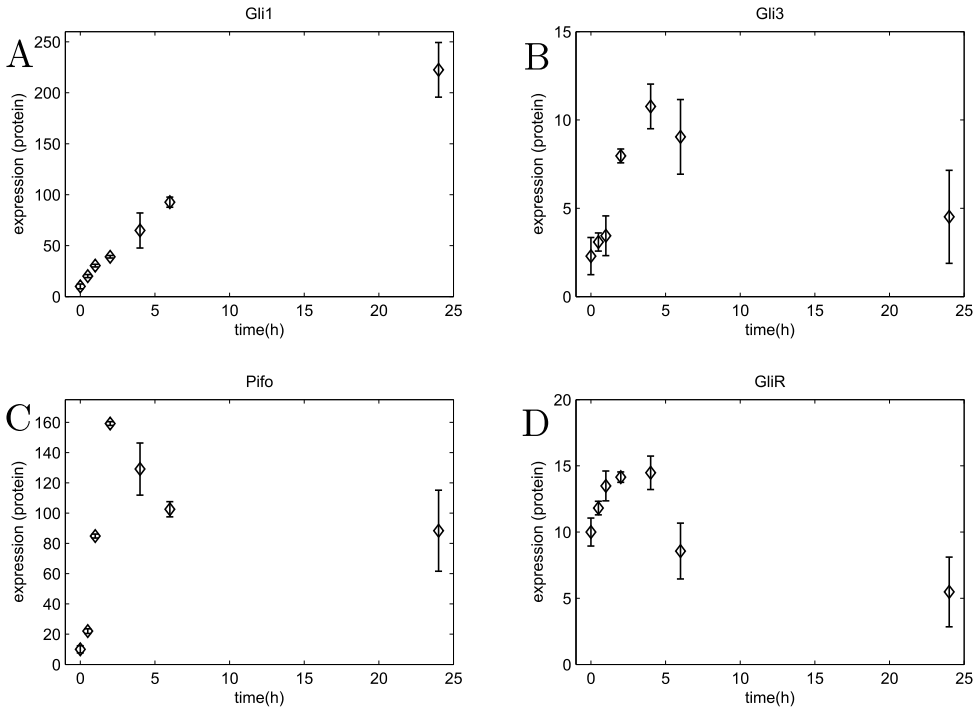

Figure 2.3: Shows the normalized and rescaled data of Gli1(A), Gli3(B), Pifo(C) and GliR(D).(A) Gli one is increasing over the whole time. But as we have no differentiation in the data between Gli1 and GliA, we can not reveal anything about a change in the equilibrium. (B) As just one time course is available for Gli3, we used the standard deviation of GliR. Because of the conservation of mass, this should cause no issues and should be accurate enough. The origin time course is used as mean. (C) For Pifo, just one time course is available as well. So we used the standard deviation of Gli1 because th data points are in the same range. The origin time course is used as mean. (D) Two time courses are available for GliR. One can see an increase of the concentration until 4h. After 4h the concentration is decreasing until 24h.

2.1.1 Normalization

For normalizing the data, we used first the RMSD (Equation 2.1) to calculate comparable time courses for Gli1 and GliR for which we have 3 and 2 respectively. So we calculated the RMSD for each time point with respect to each other data point at this time. $\vec{x_1}$ and $\vec{x_2}$ are vectors to compare. n is the count of the elements in the vectors. If we take an unbiased estimate as basis for our data, the RMSD is just the standard error which is the square root of the variance.

$$\sqrt{\frac{\sum_{i=1}^{n}(x_{1,i} - x_{2,i})^2}{n}} \tag{2.1}$$

```
1 f_RMSD(x,y) = RMSD(x,y); //calculates the RMSD between 2 points x and y
2 f_opt1(a) = f_RMSD(x, a*y); //search for the a which minimizes the RMSD between x and y
3 f_opt2(b) = f_RMSD(x, b*z); //search for the b which minimizes the RMSD between x and z
4 f_opt3(c) = f_RMSD(a*y, c*z); //search for the c which minimizes the RMSD between a*y and z
5 f_opt4(c) = mean(f_opt2(c), f_opt3(c)) // calculates the mean constant for b*z and c*z to minimize the
6 RMSD between x, y and z.
7 -> multiply y and z with the obtained constants to normalize the data
```

Listing 2.1: Using the RMSD to compare different time courses of the same protein.

To do this, we minimized the RMSD between the corresponding data points by searching for proper constants like it is shown in Listing 1. After that, we got comparable time courses which we used for the model training. Next step was to normalize the data again to the time point t_0. This is done by dividing each time point by the time point t_0. After that, we rescaled the data to 10 for easier handling. We will describe this in detail in Section 2.2.1.

2.2 Modeling

For defining and solving the ODE-models we used the SBTOOLBOX2[7] package which is available for MATLAB®. All models are derived from the literature, the meetings with our collaborators and, at the points where we had doubts, derived from the given data. For the transcription we assume for all proteins a base transcription rate. We additional use a hill function[12] where we have knowledge about the transcription factors[20]. This is not the case for Gli3 and Smo. In the case of Gli3 we can see an increasing after Shh induction at time point 0h. As we have no knowledge about the activation of Gli3, we assume a positive feedback by the Shh signal, so we use the ShhPtc-complex to model the stimulation of the Gli3 transcription. For Smo, we have even no data of the concentration in the cilium to derive a model for the transcription. So we could just assume a base transcription rate for Smo. As Gli1 is proposed to be the major transcription factor, we decided to ignore the transcriptional activity of Gli3. This also simplifies the models.

$$\theta = \frac{[L]^n}{K_d + [L]^n} \tag{2.2}$$

The Hill function is used to describe the ligand binding to a molecule. As we have here the transcription factor which binds to the DNA. $[L]$ is the concentration of unbound

ligands and the exponent n describes the cooperativity. We decided to set n to 1. This means we do not assume any cooperative behavior of the transcription factors. K_d is the dissociation constant and as we do not know this constant for our proteins, K_d is one of the parameter we try to fit.
In the cases where we haave conservation of mass, like in the case of the 'transformations' of Gli3 into GliR or Gli1 into GliA, we used a Mass action kinetic[13] (Equation 2.3). The mass action kinetic is also used for the transport from one compartment to another.

$$const = \alpha A + \beta B \rightleftharpoons \gamma C + \delta D \tag{2.3}$$

The law of mass action tells us that no matter how the equilibrium will change, the total concentration in the system remains constant. So we do not produce or lose protein by changing the equilibrium.
We first started, as mentioned before, with a very simple one compartment model (Figure 2.4). This model, we extended than to a two compartment model with the transport between cilium and cytoplasm. Both models will be described in detail in

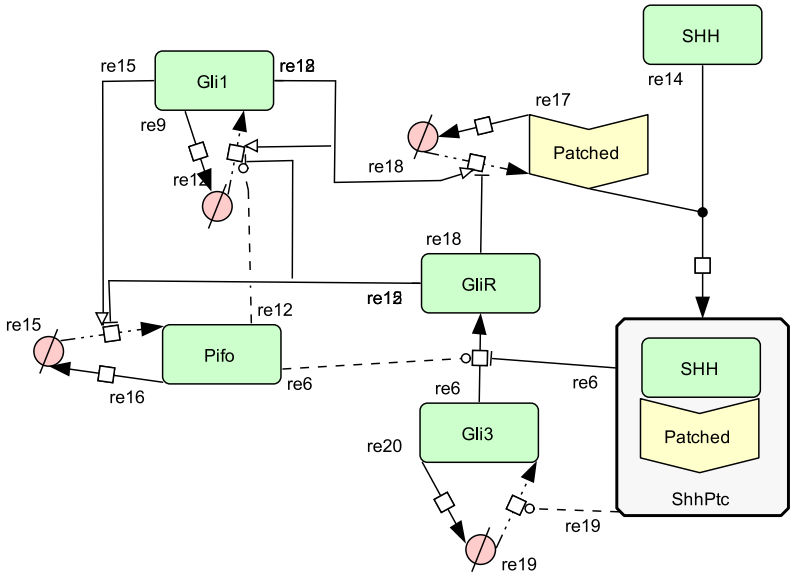

Figure 2.4: A one compartment model of the Shh signaling pathway from which we derived the final models. As Gli1 and GliR share the same targets, there is a permanent contest between these players. As we see an increase also of GliR and Gli3 after Shh induction, we assume some influence of the ShhPtc complex and Pifo onto this proteins. Also we assume an influence of Pifo onto the Shh signal, which is in this model shown by enhancing the Gli1 self activation to amplify the system.

2.2.1 Model training

The parameter training for the models is done with a simulated annealing approach[5] (see Section 2.2.2). The models were trained on the change, relative to the time point

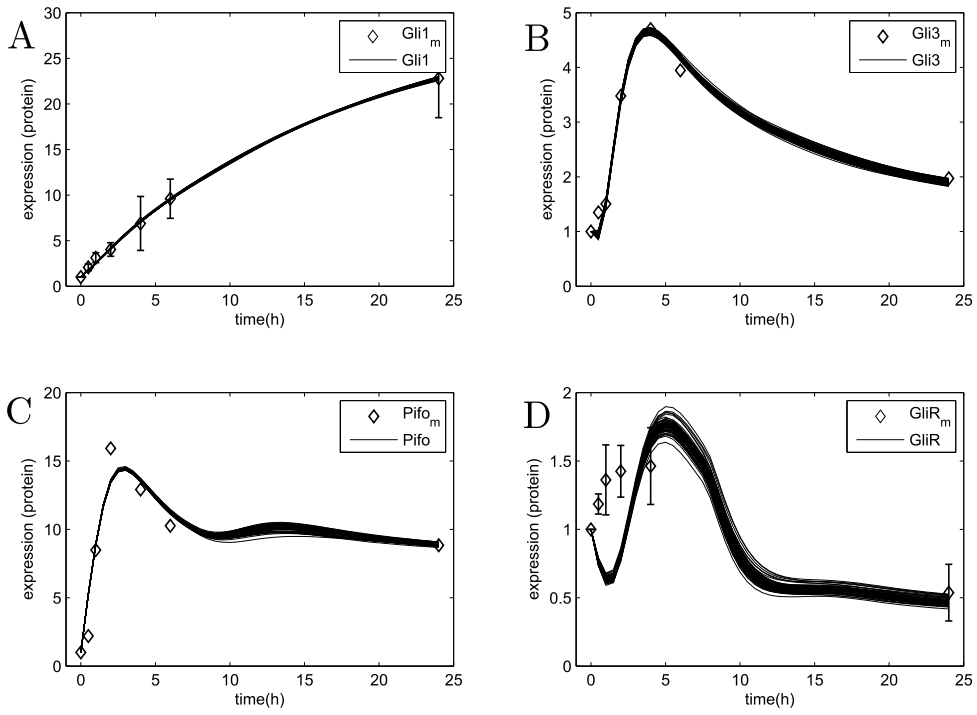

Figure 2.5: Fit of the Shh system without the pre-calculation of the base transcription rates and the normalization to fixed initial conditions. Shown is the change of the system relative to the initial value which is scaled to 1 for each protein. Shh is induced at 0h. (A) Simulation of Gli1 which fits very well. (B) Fit for Gli3. Just the data point at 0.5h is missed. (C) Fit for Pifo. The correct course of the data is reproduced. (D) Gli3 decrease in the early hours while it should increase.

t_0 ($\frac{t_i}{t_0}$). We decided to train on the change, as this is what is represented by the derivative of a function. We also rescaled the data to 10 for the time point t_0 except for Gli3, here we assumed that the Gli3 and the GliR data are comparable. So we calculated the value at which we scaled the Gli3 data from the GliR data by searching the coefficient that describes the quotient.
First we tried to fit also the initial conditions as we had no absolute molecule count. But this leads to the problem that we obtain different parameter set for the steady state and the dynamical simulation, and the system did not fall back into the steady state. This method leads to relative good fits but got stuck in a local minimum(Figure 2.5), and also did not fulfill our requirements. The system is in the steady state if the change at each time point is 0. To avoid this problem we assumed that the system starts in the steady state. To do so, we set all Shh dependent parameter and all concentrations of proteins which are not present without Shh activation to 0. The now simplified equations are set to 0 to solve it for one parameter. So we could decrease the number of parameter at the one hand, and we could be sure that our system starts in a steady state. To illustrate this, an example is given in the Equations 2.4 to 2.7

$$\frac{dGli3}{dt} = \underbrace{base3 + \alpha_6 \times (\frac{Smo_i}{\alpha_7 + Smo_i})}_{activation} - \underbrace{(\kappa_1 + \kappa_2 \times Pifo) \times Gli3}_{cleavage} - \underbrace{\beta_6 \times Gli3}_{degradation} \tag{2.4}$$

$$0 = base3 + \alpha_6 \times (\frac{Smo_i}{\alpha_7 + Smo_i}) - (\kappa_1 + \kappa_2 \times Pifo) \times Gli3 - \beta_6 \times Gli3 \tag{2.5}$$

$$0 = base3 - (\kappa_1 + \kappa_2 \times Pifo) \times Gli3 - \beta_6 \times Gli3 \tag{2.6}$$

$$base3 = (\kappa_1 + \kappa_2 \times Pifo) \times Gli3 + \beta_6 \times Gli3 \tag{2.7}$$

Figure 2.6 illustrates the switch between the steady state and the Shh activation. The parameters are random chosen. Also it is shown how the system reaches the steady state again after eliminating the Shh signal. The proteins which we assumed to be not present without Shh activation are GliA, the ShhPtc-complex, and also Smo is assumed to stay just in the cytoplasm and not in the cilium at this time.

$$\frac{\sum_{i=1}^{n}(x_{1,i} - x_{2,i})^2}{n} \tag{2.8}$$

To calculate the loss of each parameter set, we derived an error function from the mean squared error (MSE) (Equation 2.8) which is also similar the the RMSD. But we do not divide the squared error by the number of data points which are taken into account. We divide the squared error by the standard deviation σ to tolerate large error if σ is also large. If we would divide by the number of data points, we would rate an error at a protein with multiple time courses higher than the same error at a protein with just one time course.

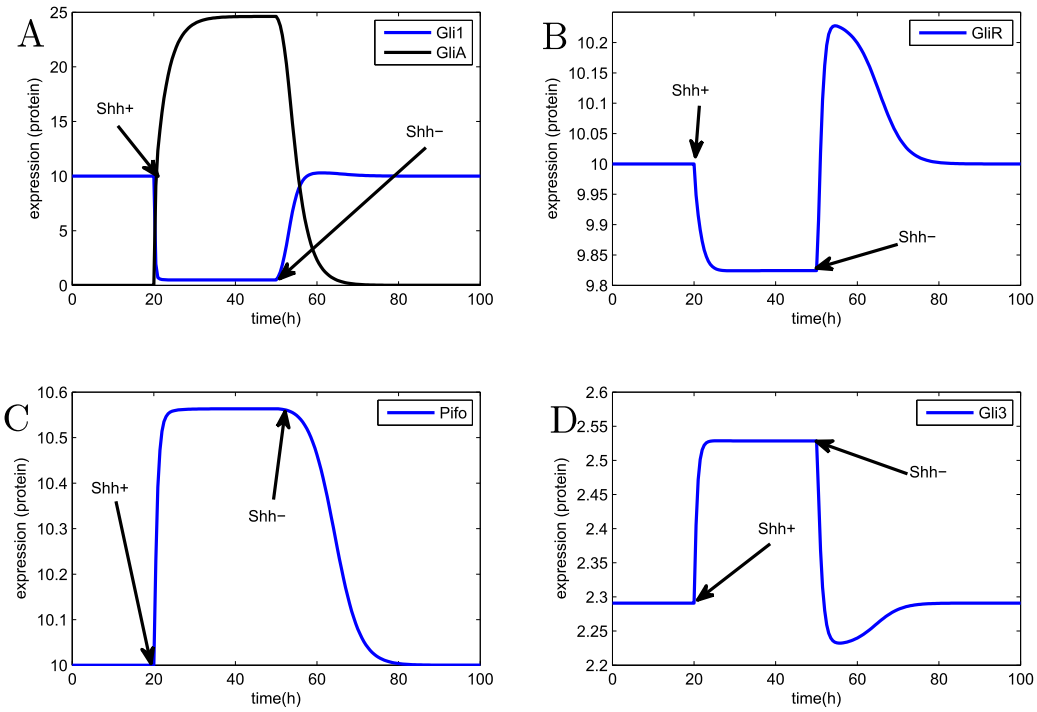

Figure 2.6: Illustration of the switch in the system by adding and removing Shh for a random parameter set. At time point 20, the Shh signal is induced, and stay active until time point 50. So as we can see all shown players reach a steady state under the shh activation, and fall back into the origin one after the Shh signal is shut down.

$$loss = \sum_{\forall x,y} \sum_{j=1}^{m} \frac{(x_i - y_i)^2}{\sigma_{x_i}} \tag{2.9}$$

We sum up over all players and over all time points. Where x_i is the mean of the measured data points at time i and y_i is the point produced by the model respectively to the given parameters. σ_{x_i} is the standard deviation of the data point x at time i. So if the standard deviation is large at this time, it produces a smaller loss if the simulated point is also farther.
For the training, we generated 1000 random parameter sets for each model as starting points and tried to fit the models with these initial parameters to the data. As cutoff for the loss (Equation 2.9), we have chosen a value of 500, which is not to selective, but also sensitive enough. The results will be shown in section Section 3.

2.2.2 Simulated annealing

Simulated annealing is a probabilistic meta heuristic for approximating a global optimum of a given function by using an adaption of the Metropolis-Hastings algorithm [5]. The goal of simulated annealing is, to find a acceptably good solution rather then the best. But in a guaranteed time.
Simulated annealing solves a problem which is described by a co-domain D, a fitness function $f : D \to \mathbb{R}$, a neighborhood $V(x)$ and a stop criterion. The first step is to choose an initial parameter set θ. We used a normal distribution $N(0, 1)$ to choose a random set of initial parameters. Now the simulated annealing changes the initial parameter set randomly until the stop criterion is reached. For each change, the algorithms decides so keep or decline the change by using the following selection.
If $f(y) \leq f(x)$ then set $x = y$ whereat x is the old parameter vector and y is the new one.
If $f(y) > f(x)$ then set $x = y$ with probability $exp\left(-\frac{f(y)-f(x)}{T_t}\right)$, whereat T_t is the actual temperature.
Here we see, if the temperature decrease, the acceptance probability decreases as well.
For our training runs, we have chosen a initial temperature of 100 to allow the acceptance also of worse parameter sets at the beginning. To also perform large changes in the parameter set, we used a logarithmic transformation for our parameter set which is shown in Equation 2.10. This function allows us not just to change a parameter in the short range given by the standard deviation, but to change the order of magnitude.

$$10^{log_{10}(\vec{x})+\mathcal{N}(\mu,\sigma)} \tag{2.10}$$

Where we define $\mu = 0$ and $\sigma = 0.3$. The standard deviation is determined by testing multiple σ.

2.2.3 Model selection

To compare the different models, we used the AIC[9] and the BIC[10] to score each model. As the models differ in the amount of parameter, it was necessary to use a criterion that

takes the number of parameter into account to compare the models. The AIC and the BIC are based on the likelihood of a model. Also it is important to take the number of parameter into account as it is possible to increase the likelihood of a model by just adding parameters. This would lead to an overfitting. Therefore, the AIC and the BIC address this problem by introducing a penalty term for the number of parameter. The penalty is larger in the BIC then in AIC. The likelihood is defined as $L(\theta) = P[x|\theta]$. So the likelihood function $L(\theta)$ of a sample is the function that assign each parameter value θ the value of the shared density function ($L(\theta) = f(x;\theta)$ (Equation 2.11).
In our case, we devised the likelihood function as a normal distribution[19]. To simplify the calculation and as both criterion uses the logarithm of the likelihood, we directly calculated the log-likelihood for each model. The function for the log-likelihood is show in Equation 2.12. The AIC and the BIC are shown in Equation 2.13 and Equation 2.14

$$L(\theta) = \int_{-\infty}^{\infty} \prod_t f(\vec{x}) d\vec{x} \tag{2.11}$$

$$\ell(\theta) = \sum_t \log\left(\frac{1}{\sigma\sqrt{2\pi}} e^{-(x-\mu)^2/2\sigma^2}\right) \tag{2.12}$$

$$AIC = 2k - 2\ln(L) \tag{2.13}$$

$$BIC = -2\ln(L) + k\ln(n) \tag{2.14}$$

k is the number of parameter and n is the number of data points used to train the model.

2.3 One compartment Model

We derived the one compartment model from the origin one shown in Figure 2.4. Because the origin one was numerically instable we had to add the activated form of Gli1. We had to do this because of the self excitation of the Gli1 protein. As we calculated the steady state, a small change of the Gli concentration lead the system out of its steady state. So the system starts to act dynamically just because of numerical errors due to the ODE-solver. By adding GliA, we now avoid this problem because GliA is just produced if the model is activated by Shh. GliA is activated by the ShhPtc-complex. We used this complex due to the assumption that there is a 1:1 relation of Ptc and Smo like it is mentioned in Section 2. So one missing Ptc in the membrane leads to one activated Smo which transduces the signal into the cell. Therefore the ShhPtc-complex should be in the same scale as Smo in the membrane. We assume the procession of the Gli family (Gli1 and Gli3) as non-reversible. So there is no back reaction in the model. In the case of Gli3 it is obvious that the reaction is non-reversible, because of the cleavage. In the case of Gli1, we also assume the phosphorylation as non-reversible so no back reaction is included. For the ShhPtc-complex we did not take a back reaction into account just to simplify the model. So after complex building, the complex degradates.

The one compartment model get along with less parameter then the two compartment model, so it should be more difficult to fit it on the one hand, but it also should be simpler

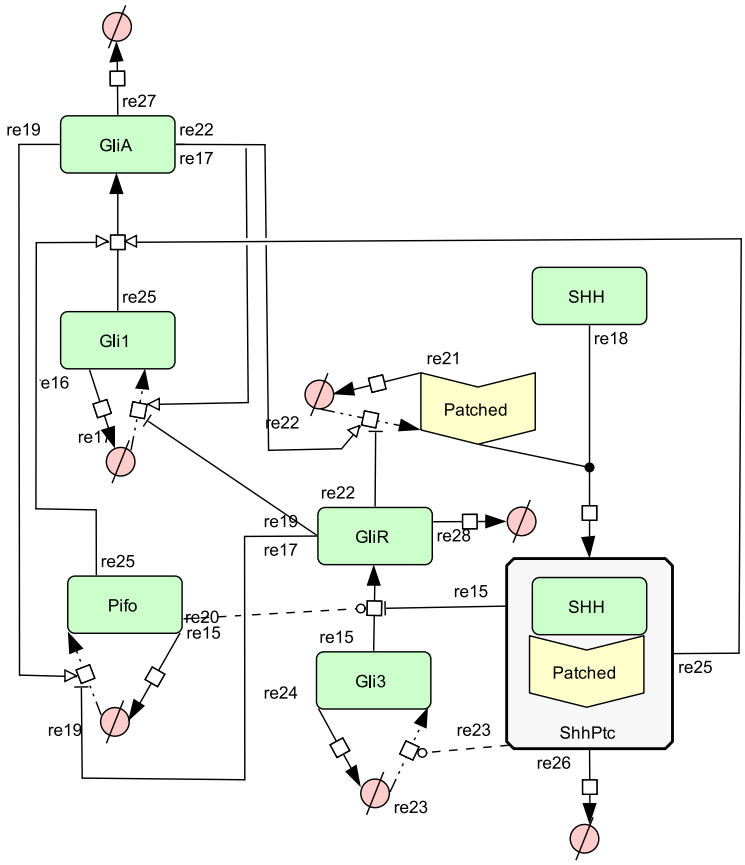

Figure 2.7: One compartment model of the sonic hedgehog signaling pathway. No compartmentation into cilium and cytoplasm is taken into account. Pifo enhances the activation of Gli1 to take into account that Pifo is important for the transport into the cilium where Gli is activated. Due to the increasing of Gli3 and GliR in the data after Shh activation, we assume also an influence of Pifo and the Shh signal on these proteins. See ODE description in Appendix 1

to find a minimum as the parameter space is smaller.

The mathematical description can be found in Appendix 1.

2.4 Two compartment Model

To test if the translocation process into the cilium is necessary, we needed also a model which provides the translocation. Therefore we created a second model with two compartments. The cytoplasm and the cilium. Here we also had the chance to test if Ptc is inhibiting the import of Smo into the plasma membrane. So we can compare the results with the results from the one compartment model which is based on the assumption that

Smo and Ptc interact directly in the membrane. Here we do not assume a 1:1 relation between Smo and Ptc. In this model, a high concentration of Ptc in the membrane should lead to a total absence of Smo in the cilium. This corresponds to the steady state, because the activator GliA is produced just by interacting with Smo in the cilium. We did not model the transport of GliA into the cilium.
With the input of Shh, Ptc is displaced. Shh and Ptc form a complex which stimulates the transcription of Gli3. Given that, the concentration of Ptc in the cilium is decreasing, so Smo can be placed there.

$$f(x) = \frac{1}{1 + exp(x)} \tag{2.15}$$

To model the dependency of Smo by Ptc, we introduced a logistic function (Equation 2.15). Logistic functions are often used to describe saturation processes. The membrane is completely saturated if the logistic function is 0. Due to the computational limitations of representing double values, this happens at a value of 710 in our arbitrary scale.

The mathematical description can be found in Appendix 2.

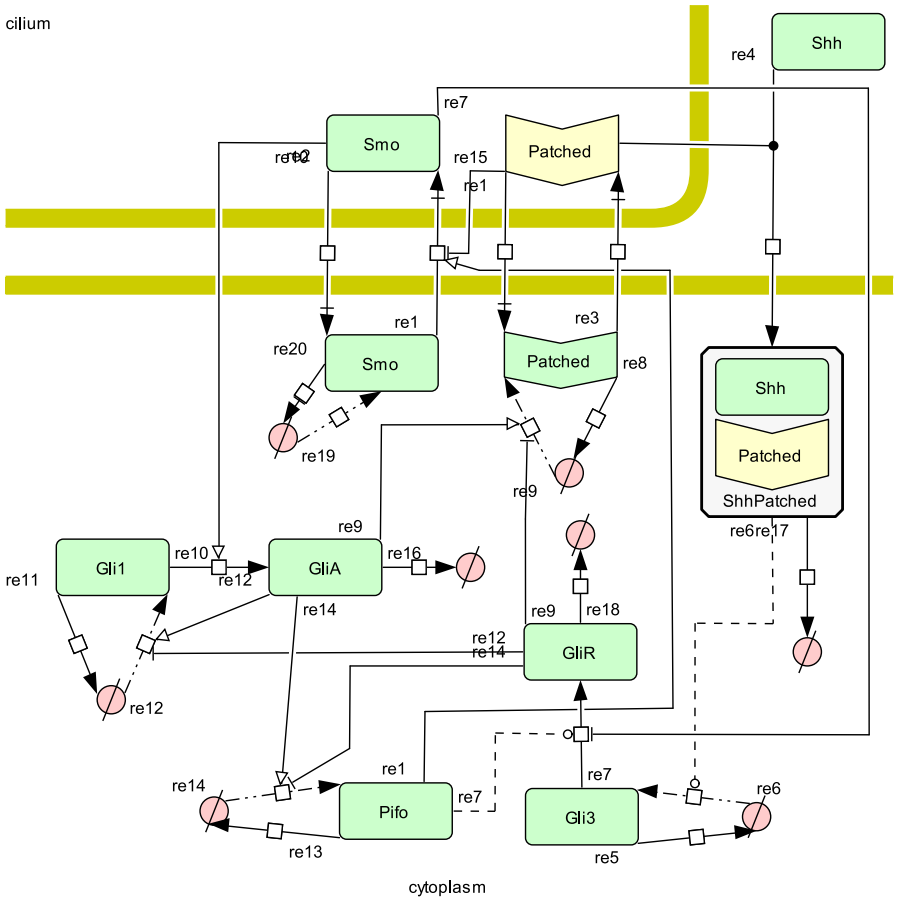

Figure 2.8: A two compartment version of the model shown in figure 2.7 including the cilium as a second compartment and Smo as the 'carrier' of the activation signal into the cell. See ODE description in Appendix 2

Chapter 3

Results

For each model, we started 1000 runs with a random parameter set which then are fitted by the simulated annealing approach. So we started with 2000 initial parameter sets. We introduced a cutoff in Section 2.2.1 of 500. This cutoff was, in the case of the one compartment model, satisfied in 15 cases. For the two compartment model, the cutoff was satisfied in 4 cases.
Interesting is, that in both cases, we obtain two 'best' parameter sets. One parameter set which provides the minimal loss calculated by the error function(we will call it 'Best loss') and one parameter sets producing the minimal AIC and also BIC value (we will call it 'Best score'). To compare both models, we used a likelihood ratio testing (Equation 3.1). All results will be shown in detail in Section 3.1 and Section 3.2.

$$x = \frac{\ell_1(\theta_1)}{\ell_2(\theta_2)} \tag{3.1}$$

Where $\ell_1(\theta_1)$ is the log-likelihood of the one compartment model with respect to the parameter set θ and ℓ_2 is the log-likelihood of the two compartment model with respect to the parameter set θ. The θ_i are the corresponding best parameter sets.

3.1 One compartment model

After 1000 runs with different initial parameter sets, 15 set satisfied the cutoff <500. The best fit produces a loss 234.5 and an AIC of 662 and a BIC of 706 (black line in Figure 3.1). The fit with the smallest AIC and BIC values produces a loss of 332.6 and an AIC of 636 and a BIC of 680 (red line in Figure 3.1). Figure 3.2 shows that the parameter sets which produce the best score (set 12) and the one producing the best score (set 2) are not in the same cluster. So we have two local minima with tolerably good results. A further step would be to investigate if one or the other minima leads to a better fit. We see a high diversity in the Gli1 time course (Figure 3.1A) after 2 to 3 hours. So the early hours are not that parameter dependent then the later hours. The same holds for Pifo (Figure 3.1C). The drop after the peak at 2 hours seems to be a key event for this protein. The time courses of Gli3 and GliR are fitted very badly, so here the model should probably

revised. The best loss parameter set yield to a good fit for Pifo and an acceptable fit for Gli1. The GliR time course is fitted just until 2h and the parameter set failed completely to fit Gli3. The parameter set which yields to the best AIC and BIC score fits the Gli1 data well but in contrast fails for Pifo. The Gli3 and GliR fits are also unacceptable.
We clustered the parameter to check whether they are correlated or not. The clustering shows what we expected, the parameter which are related in the model fall in the same cluster. For example the parameter l (λ) and b1 (β_1) are in the same cluster, this is not surprisingly as λ is the binding rate of Shh and Ptc to each other and β_1 is the degradation rate of the ShhPtc-complex. Interestingly, k2 (κ_2), which describes the rate at which Pifo enhances the Gli3 cleavage, highly correlated with g3 γ_3 which describes the repressive influence of Gli3 on the Pifo transcription, but not so high correlated with a7 (α_7) which is the transcription rate of Pifo. This could mean, that the repression γ_3 has a higher influence.

3.2 Two compartment model

Just 4 parameter sets of the 1000 initial ones yield to a loss which satisfied cutoff <500. For this model, we have also 2 interesting parameter sets, one which produce the minimal loss and one producing the minimal AIC and BIC score. All scores for the two compartment model are shown in Table 3.3. As we have just 4 parameter sets, we have a worse overview about the behavior of the system. But we can distinguish the 4 parameter sets in 2 classes. Each class contain one 'best' parameter set. The best loss parameter set (Figure 3.3 thick black lines) fits the Pifo data very well, close to over fitting, but fails in the case of Gli1, Gli3 and GliR. The best score set (Figure 3.3 thick red lines) fits the Gli1 data pretty well and also provides a fit for Pifo and GliR with the correct bias, but fails in the case of Gli3. Because just four parameter sets are available, the clustering of the parameter sets shown in Figure 3.4 has not much explanatory power. So we can not give a clear conclusion if this set of parameter sets is representative. As seen for the one compartment model, the two parameter sets producing the best loss and the best AIC/BIC score are not in the same cluster. This can also be seen in the fits. Here, a further investigation of the different minima could be the next step.
We also checked the correlation between the different parameter (Figure 3.4). Here we have a2 (α_2) as a kind of out group, and a very large cluster which ranges from a9 (α_9) to b6 (β_6) in the graphical representation shown in Figure 3.4. The correlated parameter are the same as in the one compartment model.

3.3 Comparison

The fits of both models are not that good as desirable but the right trend is observable. To compare the models, we used the AIC and BIC scores and a likelihood ratio testing. The likelihood analysis favors the simpler one compartment model, see Table 3.1. Also the AIC and the BIC scores favor the simpler one compartment model (Table 3.2 and

Table 3.3). So we have an evidence to focus more on the simple model in further research. As we compared the clustering of both model, we found an equal clustering of the parameter in both models. So, correlated parameters in the one compartment model are also correlated in the two compartment model. For example, a1 (α_1) and a8 (α_8) in the one compartment model equates to a2 (α_2) and a6 (α_6) in the two compartment model.
α_1 is the dissociation constant of the hill kinetic describing the expression of Ptc in the one compartment model like α_2 is in the two compartment model. α_8 is the transcription rate which scales the hill kinetic of Gli3 in the one compartment model like α_6 does in the two compartment model.
In general the one compartment model has a smaller but still huge parameter space, so from this point of view it is not surprising that we found more minima for the one compartment model as for the two compartment model. But still, both models have strong issues to simulate the Gli3 and GliR data but fit the Pifo data well.

one|two	Best loss	Best Score
Best loss	0.63	0.74
Best Score	0.61	0.71

Table 3.1: Ratio of the log-likelihood for the one and the two compartment model (see Equation 3.1).

	Best loss	Best Score
Loss	234.5	332.6
AIC	662	636
BIC	706	680

Table 3.2: Loss, AIC and BIC scores for the one compartment model.

	Best loss	Best Score
Loss	408	483
AIC	1045	896
BIC	1096	947

Table 3.3: Loss, AIC and BIC scores for the two compartment model.

3.4 Prediction

For each model we toke the two best parameter sets Best loss(BL) and Best score (BS) to predict the influence of Pifo onto the system. Figure 3.5 show the prediction for the one compartment model while Figure 3.6 show the prediction for the two compartment model. For both models, we see an influence of Pifo on the transcription. In the case of

Gli1, the one compartment model shows a strong reaction to the missing of Pifo, while the influence in two compartment model is not that strong. The one compartment model show no significant reactions to the absence of Pifo in the case of Gli3 and GliR. For the two compartment model, we can illustrate a weak response to the absence of Pifo for these proteins.
As the prediction show, Pifo is affecting the expression of the transcription factor Gli1. And as Gli1 is the transcription factor for the Shh target genes, Pifo also enhances the Shh signal.

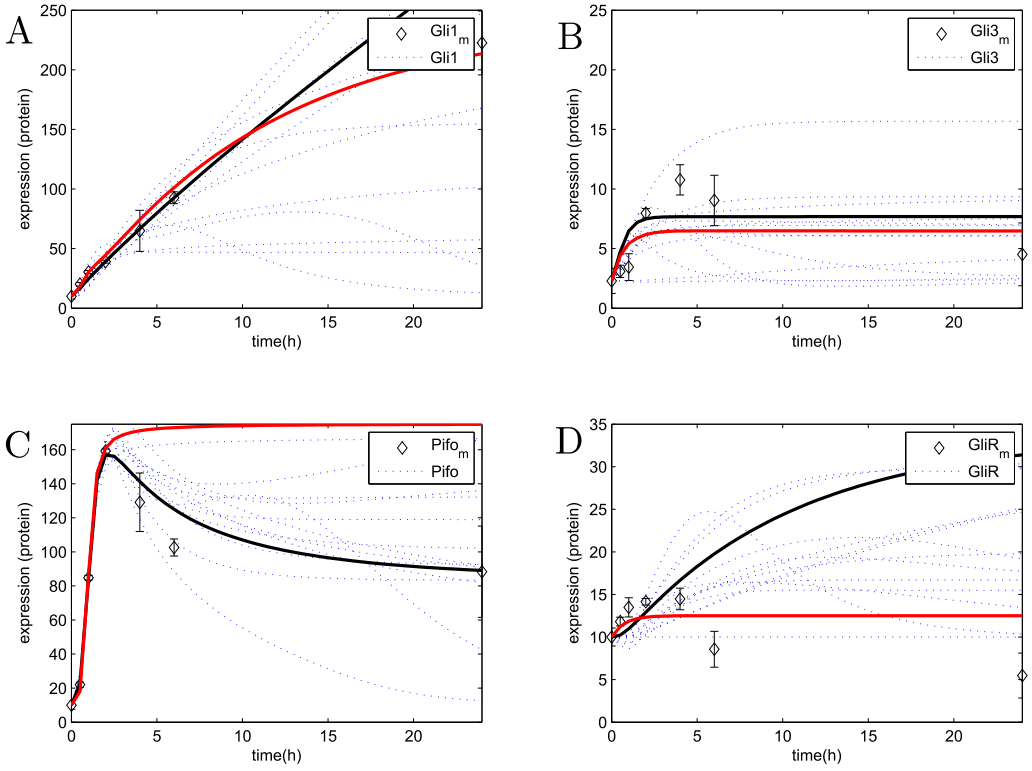

Figure 3.1: Results for the fitting of the one compartment model. Shown are all 15 parameter sets with a loss below the cutoff of 500. The black line in each subplot corresponds to the parameter set which produces the minimal loss (BL). The red line in each subplot corresponds to the parameter set which produces the minimal AIC and BIC (BS). (A)The Gli1 simulation shows very good fit for the early hour until 4h. After 4h the results starts to spread out. (B) For Gli3, mostly just a change in the level happens. The level at 24h is reached mostly because of the relative large standard deviation, but the peak at 4h is not fitted well. (C) For Pifo, we see a very nice fit until the peak at 2h, after this peak, the simulations start to diverge. (D) Shows the fit of GliR. The results differ a lot. So no parameter set is able to fit the data proper.

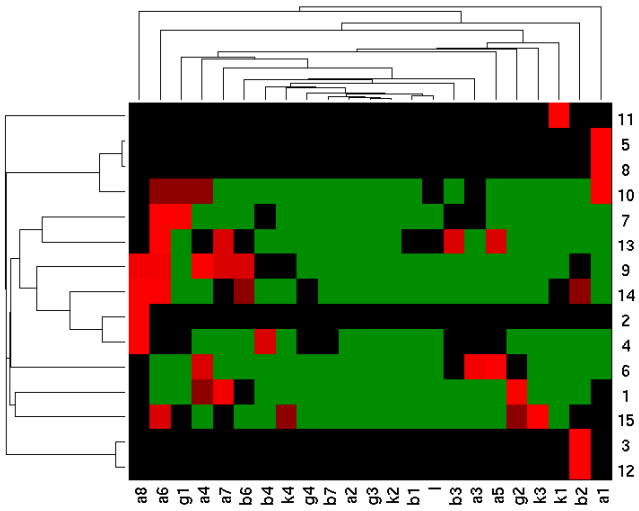

Figure 3.2: Cluster of the different parameter sets which full fill the cutoff of 500. Each line corresponds to a parameter set, while each row represents a parameter. We see five major groups. four smaller ones containing (3, 12), (15, 1, 6), (10, 8, 5) and (11) and one larger containing the most parameter sets (7, 13, 9, 14, 2 ,4). The value range is from -3 (green, negative correlated) to +3 (red, positive correlated).

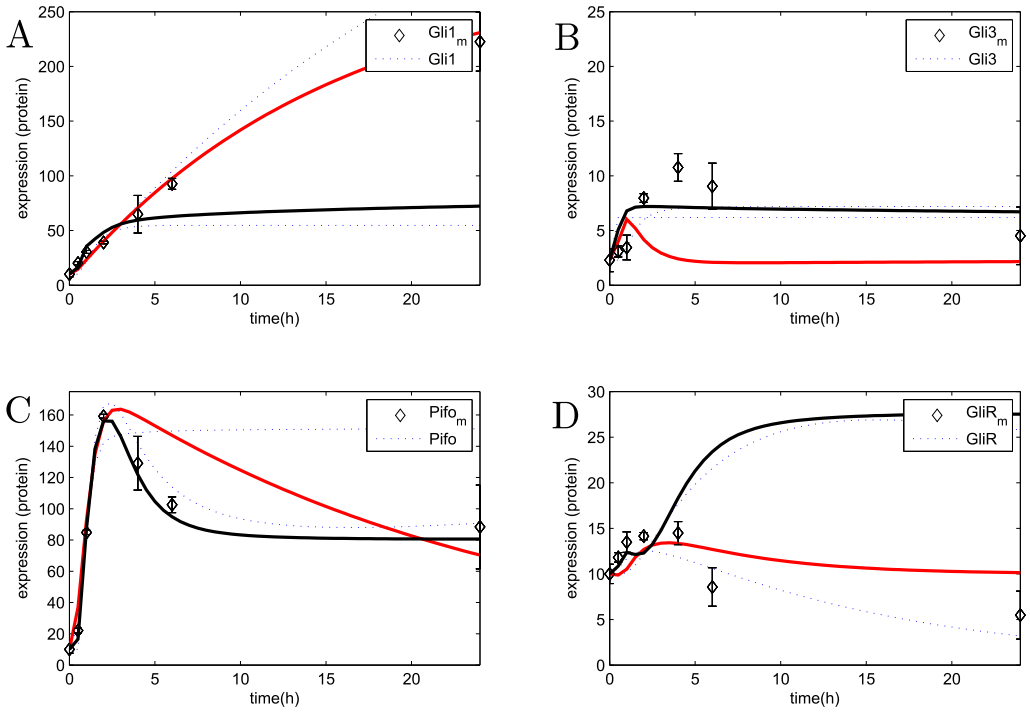

Figure 3.3: Results for the fitting of the one compartment model. Shown are all 4 parameter sets with a loss below the cutoff of 500. The black line in each subplot corresponds to the parameter set which produces the minimal loss (BL). The red line in each subplot corresponds to the parameter set which produces the minimal AIC and BIC (BS). (A) We see two separate classes each containing 2 parameter sets for Gli1. (B) The Gli3 simulation seems to fit the mean over all time points but do not follow the data. (C) Two parameter sets fit the Pifo data well while the other two not. Also here we can also distinguish two classes of parameter sets. (D) GliR also shows a clear separation into to classes of parameters. The class containing the BS set fits the data slightly while the other class, containing the BL set, is increasing until 24h.

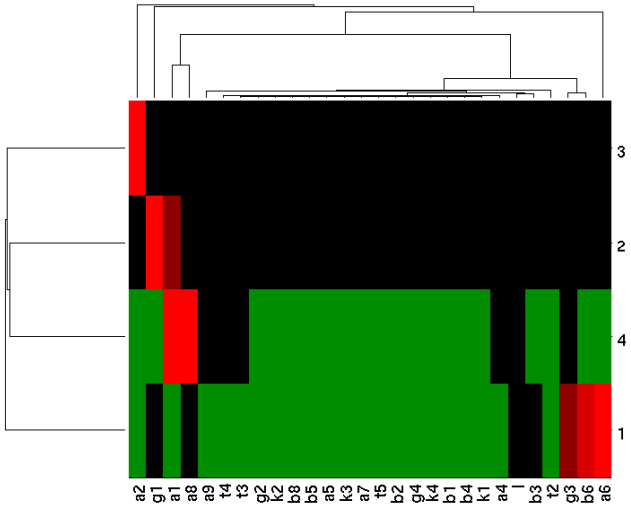

Figure 3.4: Cluster of the different parameter sets which full fill the cutoff of 500. Each line corresponds to a parameter set, while each row represents a parameter. As the sample size is to small, it is not possible to distinguish classes from this. The value range is from -3 (green, negative correlated) to +3 (red, positive correlated).

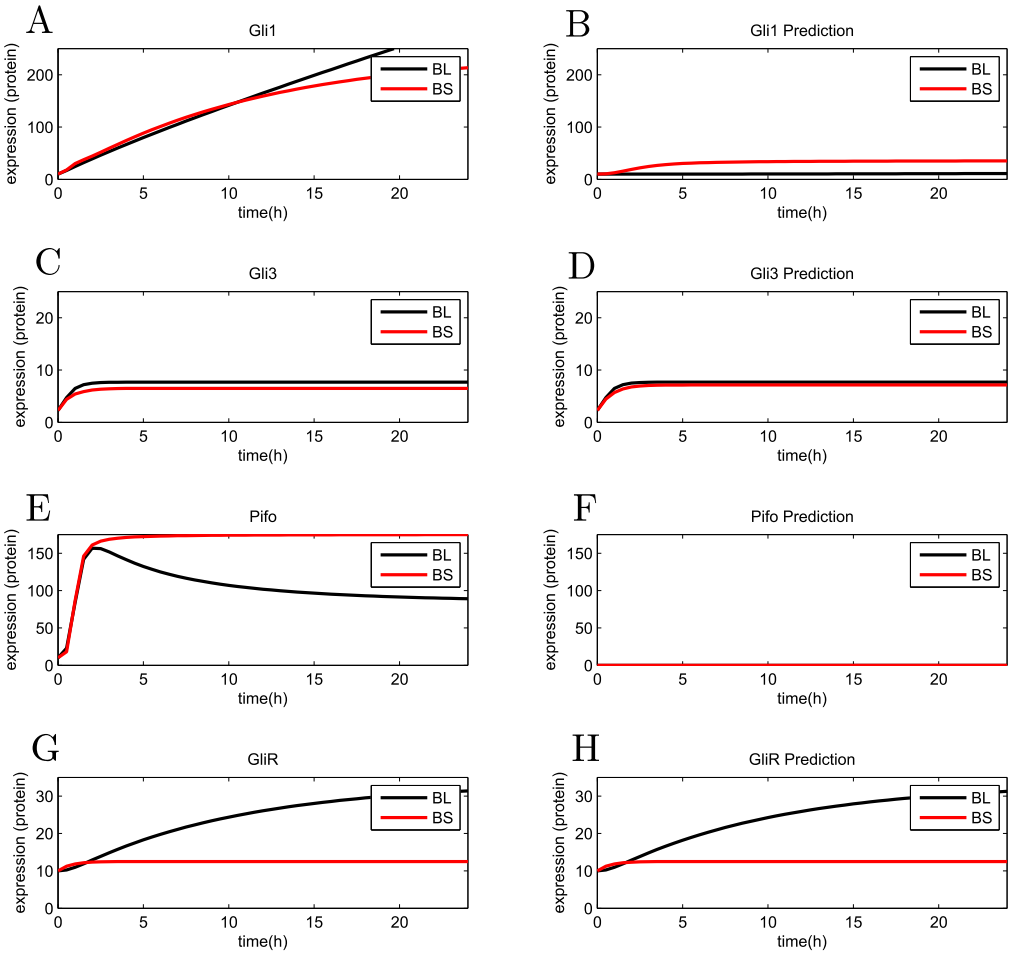

Figure 3.5: The left site (A,C,E,G) show the best fits of the one compartment model while the right site (B,D,F,H) shows the prediction where no Pifo is present. (A/B) Gli1 is in both cases affected and the expression is highly decreased. (C/D) No significant change in the concentration of Gli3 can be observed. (E/F) The Pifo expression is turned off. (G/H) Also no influence of Pifo on GliR can be observed.

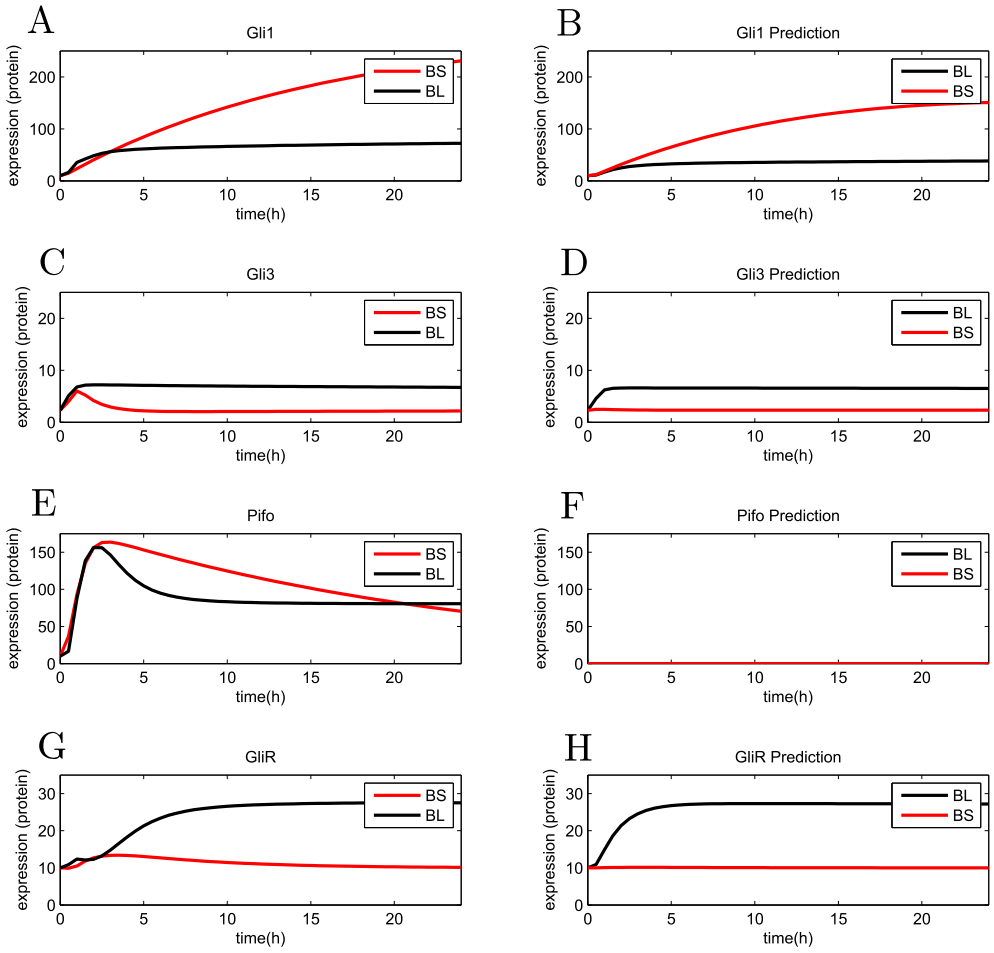

Figure 3.6: The left site (A,C,E,G) show the best fits of the one compartment model while the right site (B,D,F,H) shows the prediction where no Pifo is present. (A/B) A high expression of Gli1 is more affected than a weak expression, but in both cases the expression is reduced. (C/D) The BL set is not affected at all, but the BS set show an affection in the early hours and stay in its steady state. (E/F) The Pifo expression is turned off. (G/H) For the BL set, we see a change in the speed of reaction increases but the steady state stays the same. The BS set is affected in the opposite direction. The small increase with Pifo can not observed without Pifo. GliR stays in the origin steady state

Chapter 4

Discussion

Both models have the advantage to fit the Gli1 and Pifo data well, but also both have an issue to fit the data of Gli3 and GliR. Here we have to check whether this issue is due to the systematic shift in the GliR data which is indeed eliminated, but could cause trouble anyhow. For the one compartment model, we obtained 15 sets of parameter which fall below the chosen cutoff of 500. The 15 parameter sets belong to 5 minima as shown in Figure 3.2. For the two compartment model, we obtained 4 sets of parameter which we could not separate into different minima as the set is to small to distinguish whether they are all in the same minima or fall in four different minima (Figure 3.4). So we use a conservative approach and estimate the number of minima to the maximum. In this case we got 5 minima for the one compartment model and 4 for the two compartment model. But more realistic should be 2. We can see this in Figure 3.3 where we see two different courses each containing 2 parameter sets. This is somehow surprisingly as the number of parameter can increase the likelihood until overfitting[10].
That we got two best sets of parameter for each model is not sudden as the loss is calculated with respect to the mean of the time courses while the likelihood is calculated for each data point. So the likelihood function penalize a miss fit of Gli1, for which we have three time courses available, higher than for Pifo (just one time course available). As we obtained two best parameter sets, one fitting Gli1 well and one fitting Pifo well, for each model we should check if we can combine them to improve the fitting of the model. As we have a high correlation between the parameter sets of both models we could also include the best parameter sets of the other model respectively for improving the parameter sets. The clustering of the parameter give no support for either the one compartment model or the two compartment model as the parameter correlated in the one compartment model are also correlated in the two compartment model.
We also analyzed the behavior of the models after the Shh signal is turned off again. The one compartment model switches in one case its steady state for Pifo and Gli1(BL) and in the other case (BS) Gli1, Pifo and GliR need about 80 to 100 days to reach the origin steady state. Just Gli3 responds in both cases immediately. Here an active degradation of Gli1 or GliA - the transcription factor - may involved. As the scale is arbitrary, sadly we can not compare the concentrations of the different proteins. But we can see that Gli1 (BS) is still increasing while the concentration of GliA is decreasing. Pifo decreases

immediately after the Shh signal is shut off, but stay for about 500h at a higher level before it converge against the origin steady state.
The two compartment model show a comparable behavior. But here also GliR responds in both cases (BL and BS) directly the the absence of Shh. For the parameter set BS, also Gli1 and Pifo respond directly to the absence of Shh. For Gli3 and GliR we see a fall back into the steady state before the Shh signal is turned off. But if we look at the data, in both cases, we see a peak at 4h and a decreasing concentration until 24h. While the concentration of Gli1 is increasing and the one of Pifo remains nearly constant. So the decrease of Gli3 and GliR could be reasonable. So Gli3 and GliR may affected just direct after Shh induction. For the BL parameter set, the Gli1 and Pifo and also the GliA concentration decrease very slowly. This could also be an evidence for an active degradation. As both models have an issue to fit the data of Gli3 and GliR, it may be necessary to also include the minor transcription factor Gli3A, the activated form of Gli3. But as the AIC, BIC and also the likelihood ratio test support the one compartment model, we will focus on this model in further research. So we could show that it is not necessary to model the compartmentation.

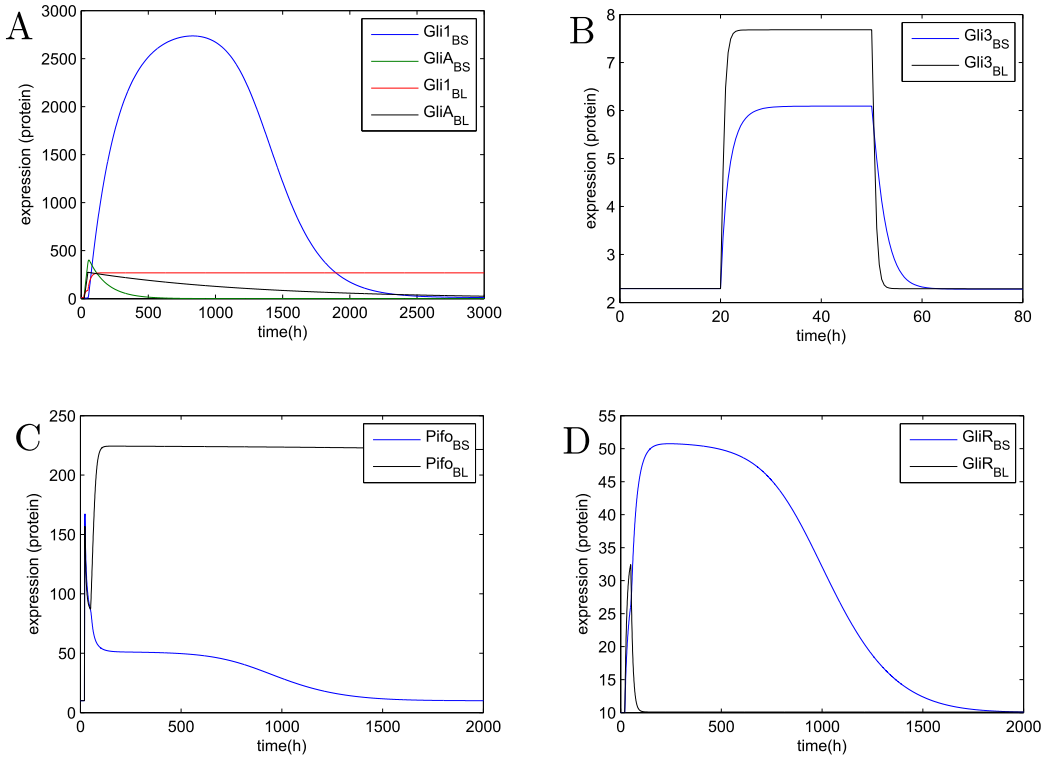

Figure 4.1: Analysis of the fall back after the Shh signal is turned off for the two obtained parameter sets of the one compartment model. BS means the Best score parameter set, and BL means the Best loss set. Shh is activated at 20h and is deactivated at 50h. (A)For the BS set, Gli1 needs about 100 days to fall back to the steady state. For the BL set, Gli1 falls in a different steady state. (B) In both cases, Gli3 responds immediately to the absence of Shh. (C) For Pifo we see the same behavior like for Gli1. (D) GliR also needs around 100 days to fall back into the steady state for the BS set. The BL set responds directly.

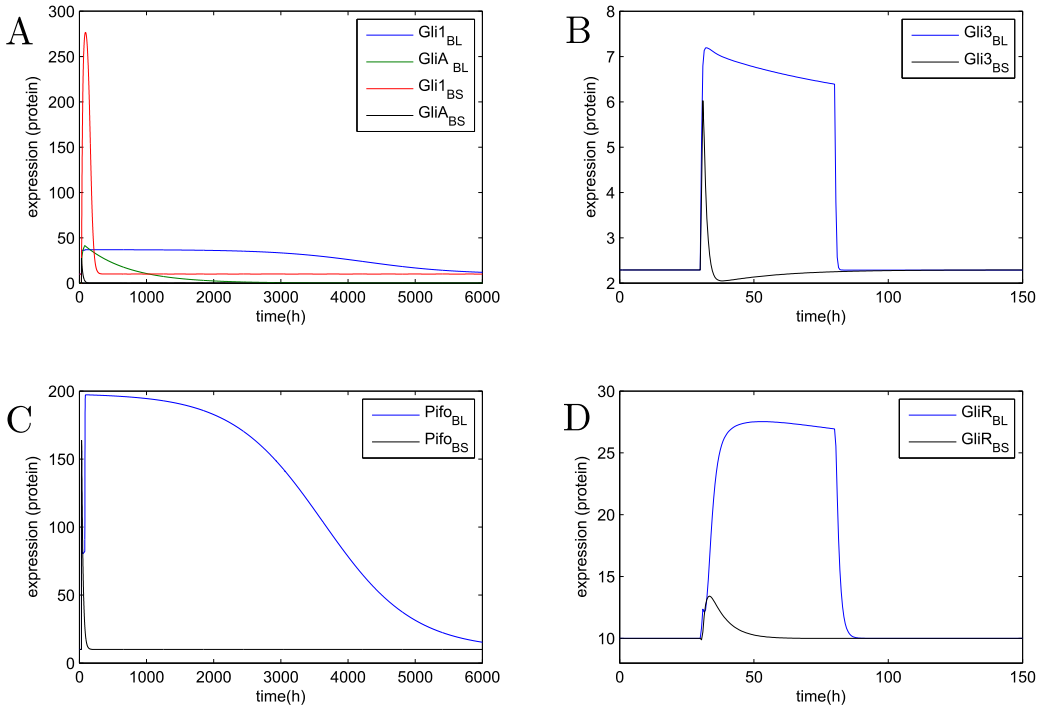

Figure 4.2: Analysis of the fall back after the Shh signal is turned off for the two obtained parameter sets of the one compartment model. BS means the Best score parameter set, and BL means the Best loss set. Shh is activated at 20h and is deactivated at 80h. (A) The BS set react directly onto the missing Shh signal, while the BL set needs around 250 days to fall back into the steady state. (B) The BL set increases Gli3 rapidly at the activation, and is then slowly decreasing over time. At the deactivation of the Shh signal, Gli3 drops rapidly back to the steady state. The BS set provides just a peak at the activation, and a rapid decrease. The concentration then is increasing again over time until it reaches the steady state. (C) Pifo shows for both sets, BL and BS, the same behavior as Gli1 which is not surprisingly, as the transcription of Pifo is regulated by Gli1 in the same way like the Gli1 activation itself. (D) For GliR, we see the same behavior for both sets, BL and BS as for Gli3. But in the case of BS, the drop is not so strong.

Chapter 5

Conclusion and Outlook

Pifo is argued to be important for ciliary trafficking. We created two quantitative ODE models to simulate the sonic hedgehog signaling pathway to investigate the role of Pifo in the pathway. Both model are derived from literature and experimental data. As there is no knowledge about the Gli3 activation, we derived a own interpretation of the Gli3 activation from the data. A simulated annealing approach was used to fit the parameter onto the experimental data. For the model and parameter comparison, the likelihood of the two best parameter sets for each model of was calculated. The simulations show a good understanding about, how Pifo is present in the cell, which regulatory mechanism act on Pifo. We could also show, with a prediction for both models, that Pifo enhances the sonic hedgehog signal. This was done by turning Pifo off and compare the results with the best parameter sets obtained from the simulated annealing. A further step should be, to fit the models also on the knockout data. Here, it would be interesting to investigate what consequences different concentrations of Pifo and Shh have on the expression of the target genes. Which influence has the strength of the Shh signal on the system. Does a smaller concentration of Pifo require a stronger Shh signal? As Ptc inhibits its own transcription by a negative feedback loop and also the transcription of the other Shh target genes indirect, Margio et. al propagated that Ptc in the cilium has to be inhibited completely to start the transcription. So in cells with an overexpression of Ptc, the Shh signal is no longer sufficient to completely antagonize the function of Ptc [16]. This is currently not done due to the issues which came up by fitting the models. The results show that both models have indeterminacies in the parameter. In both cases, two parameter sets came up. One producing the best loss of the error function, and one providing the best AIC and BIC scores. So to determine whether one set is more likely or not, a Bayesian sampling or a profile-likelihood method could be applied like it is proposed by Venzon et. al to avoid the problem that the properties of a parameter set θ can differ a lot from the asymptotic properties if the sample size is small[18].

Appendix 1

$$\frac{dShhPtc}{dt} = ShhPtc_{aufbau} - ShhPtc_{abbau}$$

$$\frac{dPtc}{dt} = Ptc_{aufbau} - ShhPtc_{aufbau} - Ptc_{abbau}$$

$$\frac{dGli}{dt} = Gli_{aufbau} - GliA_{aufbau} - Gli_{abbau}$$

$$\frac{dGliA}{dt} = GliA_{aufbau} - GliA_{abbau}$$

$$\frac{dGli3}{dt} = Gli3_{aufbau} - GliR_{aufbau} - Gli3_{abbau}$$

$$\frac{dPifo}{dt} = Pifo_{aufbau} - Pifo_{abbau}$$

$$\frac{dGliR}{dt} = GliR_{aufbau} - GliR_{abbau}$$

$$ShhPtc_{aufbau} = \lambda_1 \times Shh \times Ptc$$

$$ShhPtc_{abbau} = \beta_1 \times ShhPtc$$

$$Ptc_{aufbau} = base_1 + \alpha_5 \times (\frac{GliA}{\alpha_1 + GliA}) \times (1 + (\frac{1}{\gamma_1 \times GliR}))$$

$$Ptc_{abbau} = \beta_2 \times Ptc$$

$$Gli_{aufbau} = base_2 + \alpha_6 \times (\frac{GliA}{\alpha_2 + GliA} \times (1 + \frac{1}{\gamma_2 \times GliR}))$$

$$Gli_{abbau} = \beta_3 \times Gli$$

$$GliA_{aufbau} = \kappa_3 \times ShhPtch \times Pifo \times Gli + \kappa_4 \times ShhPtch \times Gli1$$

$$GliA_{abbau} = \beta_7 \times GliA$$

$$Gli3_{aufbau} = base_3 + \alpha_8 \times \frac{ShhPtc}{\alpha_3 + ShhPtc}$$

$$Gli3_{abbau} = \beta_4 \times Gli3$$

$$Gli3_{cleavage} = (\kappa_1 + \kappa_2 \times Pifo) \times Gli3$$

$$GliR_{repression} = 1 + \gamma_4 \times ShhPtc$$

$$GliR_{aufbau} = \frac{Gli3_{cleavage}}{GliR_{repression}}$$

$$GliR_{abbau} = \beta_5 \times GliR$$

$$Pifo_{aufbau} = base_4 + \alpha_7 \times (\frac{GliA}{\alpha_4 + GliA}) \times (1 + (\frac{1}{\gamma_3 \times GliR}))$$

$$Pifo_{abbau} = \beta_6 \times Pifo$$

Appendix 2

$$\frac{dShhPtc}{dt} = ShhPtc_{binding} - ShhPtc_{abbau}$$

$$\frac{dPtc_i}{dt} = Ptc_{transIn} - ShhPtc_{binding} - Ptc_{transOut}$$

$$\frac{dPtc_y}{dt} = Ptc_{y_{aufbau}} + Ptc_{transOut} - Ptc_{transIn} - Ptc_{y_{abbau}}$$

$$\frac{dSmo_i}{dt} = Smo_{transIn} - Smo_{transOut}$$

$$\frac{dSmo_y}{dt} = Smo_{y_{aufbau}} + Smo_{transOut} - Smo_{transIn} - Smo_{y_{abbau}}$$

$$\frac{dGli1}{dt} = Gli_{aufbau} - GliA_{aufbau} - Gli_{abbau}$$

$$\frac{dGliA}{dt} = GliA_{aufbau} - GliA_{abbau}$$

$$\frac{dGli3}{dt} = Gli3_{aufbau} - Gli3_{cleavage} - Gli3_{abbau}$$

$$\frac{dPifo}{dt} = Pifo_{aufbau} - Pifo_{abbau}$$

$$\frac{dGliR}{dt} = GliR_{aufbau} - GliR_{abbau}$$

$$ShhPtc_{binding} = \lambda_1 \times Ptc_i \times Shh$$

$$ShhPtc_{abbau} = \beta_1 \times ShhPtc$$

$$Ptc_{y_{aufbau}} = base1 + \alpha_1 \times (\frac{GliA}{\alpha_2 + GliA} \times (1 + \frac{1}{\gamma_1 \times GliR}))$$

$$Ptc_{y_{abbau}} = \beta_2 \times Ptc_y$$

$$Ptc_{transIn} = \tau_1 \times Ptc_y$$

$$Ptc_{transOut} = \tau_2 \times Ptc_i$$

$$Smo_{y_{aufbau}} = \alpha_3$$

$$Smo_{y_{abbau}} = \beta_3 \times Smo_y$$

$$Smo_{transIn} = \tau_3 \times f(Ptc_i) \times Pifo \times Smo_y$$

$$Smo_{transOut} = \tau_4 \times Smo_i$$

$$Gli_{aufbau} = base2 + \alpha_4 \times (\frac{GliA}{alpha5 + GliA} \times (1 + \frac{1}{\gamma_2 \times GliR}))$$

$$Gli_{abbau} = \beta_4 \times Gli1$$

$$GliA_{aufbau} = \kappa_1 \times Smo_i \times Pifo \times Gli1 + \kappa_2 \times Smo_i \times Gli1$$
$$GliA_{abbau} = \beta_5 \times GliA$$

$$Gli3_{aufbau} = base3 + \alpha_6 \times \frac{Smo_i}{\alpha_7 + Smo_i}$$
$$Gli3_{cleavage} = (\kappa_3 + \kappa_4 \times Pifo) \times Gli3$$
$$Gli3_{abbau} = \beta_6 \times Gli3$$

$$GliR_{repression} = 1 + \gamma_4 \times Smo_i$$
$$GliR_{aufbau} = \frac{Gli3_{cleavage}}{GliR_{repression}}$$
$$GliR_{abbau} = \beta_7 \times GliR$$

$$Pifo_{aufbau} = base4 + \alpha_8 \times (\frac{GliA}{\alpha_9 + GliA} \times (1 + \frac{1}{\gamma_3 \times GliR}))$$
$$Pifo_{abbau} = \beta_8 \times Pifo$$

The i stands for the protein in the cilium, and the y for for the protein in the cytoplasm.

List of Figures

List of Tables

Bibliography

[1] Philip W. Ingham, Andrew P. McMahon *Hedgehog signaling in animal development: paradigms and principles.* Cold Spring Harbor Laboratory Press 2001

[2] Doris Kinzel, Karsten Boldt, Erica E. Davis, Ingo Burtscher, Dietrich Trümbach, Bill Diplas, Tania Attié-Bitach, Wolfgang Wurst, Nicholas Katsanis, Marius Ueffing and Heiko Lickert *Pitchfork Regulates Primary Cilia Disassembly and Left-Right Asymmetry.* Science Direct 2010

[3] Scorr F. Gilbert *Developmental Biology. 6th edition* Sinauer Associates 2000

[4] Fiona Simpson, Markus C Kerr, Carol Wicking *Trafficking, development and hedgehog* Science Direct 2009

[5] S. Kirkpatrick, C. D. Gelatt, Jr. and M. P. Vecchi *Optimization by Simulated Annealing* Science 1983

[6] Eisenmann, D. M., *Wnt signaling* (June 25, 2005), WormBook, ed. The C. elegans Research Community, WormBook, doi/10.1895/wormbook.1.7.1, http://www.wormbook.org.

[7] Schmidt, Henning and Jirstrand, Mats *Systems Biology Toolbox for MATLAB: A computational platform for research in Systems Biology*, Bioinformatics, 22(4), 514-515, 2006. (www.sbtoolbox2.org)

[8] Kitano, H.et al. *Using process diagram for the graphical representation of biological networks*, Nature Biotechnology 23(8), 961-966 (2005)

[9] Hirotugu Akaike: *Information theory and an extension of the maximum likelihood principle.* In: B. N. Petrov (Hrsg.) u.A.: Proceedings of the Second International Symposium on Information Theory Budapest: Akademiai Kiado 1973. S. 267-281

[10] Schwarz, G. *Estimating the dimension of a model.* Ann. Statist.,5, 461464 1978

[11] Sangdun Choi *Systems Biology of Signaling Networks* Springer 2010

[12] B. Mitavskiy, D. Chu, and Radu Zabet. *Models of transcription factor binding: Sensitivity of activation functions to model assumptions.* Journal of Theoretical Biology 257 (3): 419429 2009

[13] F. Horn und R. Jackson *General mass action kinetics* Springer 1972

[14] John W. Pratt (May 1976). *F. Y. Edgeworth and R. A. Fisher on the Efficiency of Maximum Likelihood Estimation.* The Annals of Statistics 4 (3): 501514.

[15] Jain E., Bairoch A., Duvaud S., Phan I., Redaschi N., Suzek B.E., Martin M.J., McGarvey P., Gasteiger E. *Infrastructure for the life sciences: design and implementation of the UniProt website.* BMC Bioinformatics, 10:136 (2009).

[16] V Marigo and C J Tabin *Regulation of patched by sonic hedgehog in the developing neural tube.* PNAS 1996 93: 9346-9351.

[17] Karen Lai, Matthew J. Robertson, and David V. Schaffer *The Sonic Hedgehog Signaling System as a Bistable Genetic Switch* Biophysical Journal Volume 86 May 2004 27482757

[18] D.J. Venzon and S.H. Moolgavkar *A Method for Computing Profile-Likelihood-Based Confidence Intervals* Journal of the Royal Statistical Society 1987

[19] A.C. Davidson *Cambridge series in Statistical and Probabilistic Mathematics* Cambridge University Press 2003

[20] Ansorg M, Blöchl F, zu Castell W, Theis FJ and Wittmann DM. *Gene regulation at the mid-hindbrain boundary: Study of a mathematical model in the stationary limit*, Int J Biomath and Biostat, International Journal for Biomathematics and Biostatistics 1, 2010.